

## THE CONDUCTANCE OF SODIUM CHANNELS UNDER CONDITIONS OF REDUCED CURRENT AT THE NODE OF RANVIER

BY F. J. SIGWORTH

*From the Department of Physiology, Yale School of Medicine,  
New Haven, Connecticut 06510, U.S.A.*

*(Received 11 July 1979)*

### SUMMARY

1. The single sodium channel conductance  $\gamma$  and the number of channels  $N$  were estimated from fluctuation analysis in voltage-clamped nodes of Ranvier under conditions that decreased the size of the sodium current.

2. Reduction of the sodium current by depolarizing prepulses had no effect on  $\gamma$ , and, in cases where it could be determined, had no significant effect on  $N$ . Partial block of the sodium conductance with tetrodotoxin and saxitoxin also did not affect  $\gamma$  significantly, but reduced  $N$ .

3.  $\gamma$  was reduced to about 40% of the control value at  $-5$  mV when the pH of the external solution was reduced to 5.0. The pH dependence of  $\gamma$  is consistent with the theories of Woodhull and of Drouin & Neumcke.

4. The differing effects of prepulses, toxins and pH are interpreted in view of the different time scales of channel inactivation or block under these conditions.

5. The nearly unchanged  $\gamma$  with prepulses and partial toxin block provides further evidence for the absence of interactions among sodium channels.

### INTRODUCTION

The previous paper detailed a method for determining the single channel current  $i$  and the number of sodium channels  $N$  in a node of Ranvier from fluctuations in the sodium current. This paper describes the effect on  $\gamma$  and  $N$  of various conditions that reduce the magnitude of the sodium current. One motivation of this work was to test for interactions among channels. To do this, the effect on  $\gamma$  of the degree of inactivation or toxin block of the channels was studied. Changes in  $\gamma$  would be expected if there were interactions among channels that caused correlations in the gating of one channel with the gating of another. A second motivation for studying changes in  $\gamma$  was to discriminate between gating and permeation effects in the block of sodium currents at low pH.

### METHODS

The experiments described in this paper were performed concurrently with those of the previous one (Sigworth, 1980), using the same fibres whose parameters were given in Table 1.

Present address: Max Planck Institut für Biophysikalische Chemie, D-3400 Göttingen, Postfach 968, West Germany.

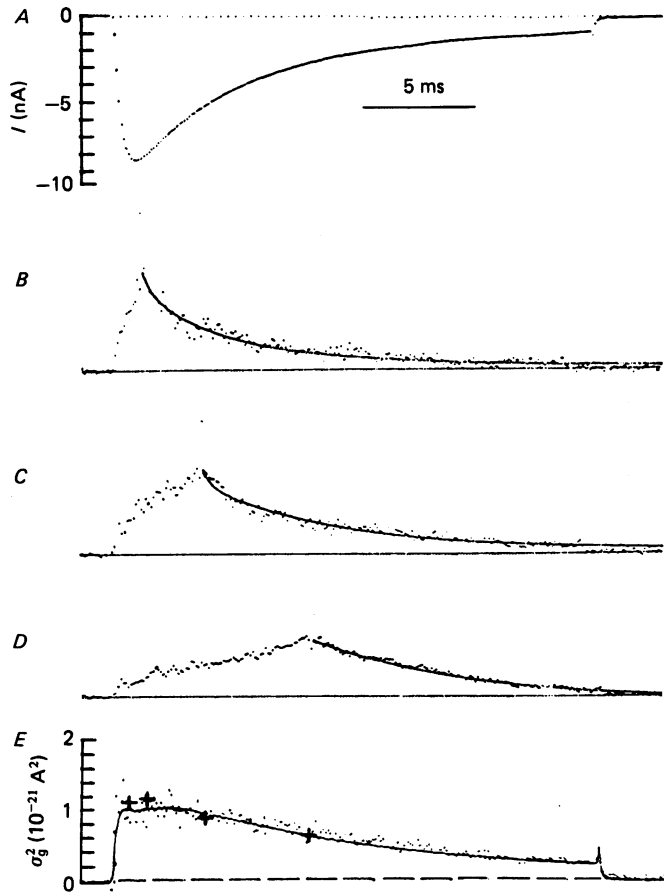


Fig. 1. Comparison of covariance peaks with the corrected variance. *A*, mean current from 20 ms depolarizations to  $-5$  mV with 50 ms prepulses to  $-105$  mV. *B*, *C*, *D*, covariance function  $c(t_1, t_2)$  evaluated at  $t = 1.5$ ,  $3.9$  and  $8.2$  ms after the start of the depolarizations, plotted as a function of  $t_1$ . Continuous curves are sums of three exponential functions with time constants  $6.4$ ,  $2.1$  and  $0.3$  ms, selected to provide a good (but not necessarily unique) fit to the time course in *A*. The amplitudes of the three components were varied to fit the falling phase of each projection. *E*, time course of the corrected variance  $\sigma_g^2$ . The smooth curve is the prediction with  $i = 0.3$  pA and  $N = 43,000$ . The crosses mark the peak values of the fitted curves in *B*, *C*, and *D*, and one additional fit (not shown). Node 19; 100 groups of four depolarizations.

For the toxin experiments, nanomolar concentrations of tetrodotoxin (TTX) or saxitoxin (STX) were added to the standard Ringer solution which contained 20 mM-tetraethylammonium ion. For the pH experiments a solution having increased buffering capacity was used. It contained (concentrations in mM) 87 NaCl, 20 TEA-Cl, 2 CaCl<sub>2</sub>, 5 HEPES and 5 propionate, titrated with HCl.

As before, voltage-clamped nodes of Ranvier were depolarized repetitively and fluctuations among the elicited currents were analysed. In the previous paper the relationship

$$\sigma_g^2 = iI - \frac{1}{N}I^2 \quad (1)$$

between the corrected variance  $\sigma_g^2$  and the mean current  $I$  was fitted by eye. In the present work a least-squares procedure was used instead to determine both values and error estimates for the single channel current  $i$  and the number of channels  $N$ . In the fitting procedure, the statistical error in  $i$  and  $N$  was also estimated. At low pH and when depolarizing prepulses were given, the peak fraction of channels open  $p_{\max}$  was often smaller than about 0.3 and the determination of  $N$  was subject to a large uncertainty. In these situations the fitting was constrained with  $N$  assigned its control value for that node. Values of the single-channel chord conductance  $\gamma$  were calculated from  $\gamma = i/(E - E_{Na})$ , where the test potential  $E$  was  $-5$  mV and  $E_{Na}$  is the reversal potential.

Although several determinations of  $N$  and  $\gamma$  were made for each fibre, for comparison with conditions that decreased  $I$  the control values obtained immediately beforehand were used. In some experiments considerable time had elapsed since the initial determinations of  $\gamma$  and  $N$ . For example, node 24 had been voltage-clamped for 2 h before the data of Fig. 3 was taken. For this reason the control values sometimes differ slightly from the values in Table 1 of the preceding paper.

Covariance functions

$$c(t_1, t_2) = \langle x(t_1) x(t_2) \rangle$$

were also calculated, with  $x(t)$  being the fluctuation in the observed current  $y(t)$ ,

$$x(t) = y(t) - I(t)$$

In some cases the variance  $\sigma_g^2$  was obtained from fits to three or four projections of the covariance, rather than from the direct calculation of the total variance with correction for the thermal noise background. Fig. 1 illustrates this method. Since the thermal noise contributes only a narrow spike at  $t_1 = t_2$  in the covariance, the extrapolated peak value of the more slowly varying components of the covariance is expected to be the variance from channel gating fluctuations. Part *E* of the Figure shows that the extrapolations agree well with the directly calculated variance, after it is corrected for the background.

Estimation of the variance from the covariance was done in some of the experiments because of an artifact. Unfiltered high-frequency noise components in the current-monitor signal sometimes caused the variable-gain amplifier that precedes the low-pass filter to approach its slow-rate limit when it was set for high gains. This increased the background noise within the filter band width to 50–100% more than predicted for the thermal noise, and caused the directly-calculated variance to be in error. The additional noise was essentially 'white' within the filter band width, however, and the slowly varying part of the covariance was apparently unchanged, so I chose to obtain the variance values from the covariance in those cases.

## RESULTS

*Reduction of  $I_{Na}$  with prepulses.* Depolarizing prepulses reduce the size of the sodium current but do not affect the single-channel conductance. Fig. 2*A* shows variance-mean plots from node 38, where two sets of depolarizations using different prepulses were given. The same values for the parameters  $N$  and  $i$  were used to generate the theoretical curves, which provide acceptable fits. The relative  $\gamma$  values obtained from least-square fits from six fibres are shown in part *B* of the Figure. Values of  $\gamma$  obtained with 50 ms prepulses to between  $-71$  and  $-55$  mV were divided by control values obtained with  $-30$  mV prepulses, and the ratio is plotted as a function of the relative size of the peak currents. No significant change in  $\gamma$  was seen as the peak current was reduced.

The variance-mean relationships were consistent with  $N$  being unaffected by prepulses. Determinations of  $N$  by fitting eqn. (1) generally had large uncertainties when depolarizing prepulses were used. In node 39, however, an unconstrained fit was possible. With prepulses to  $-65$  mV the peak current was reduced to 43% of

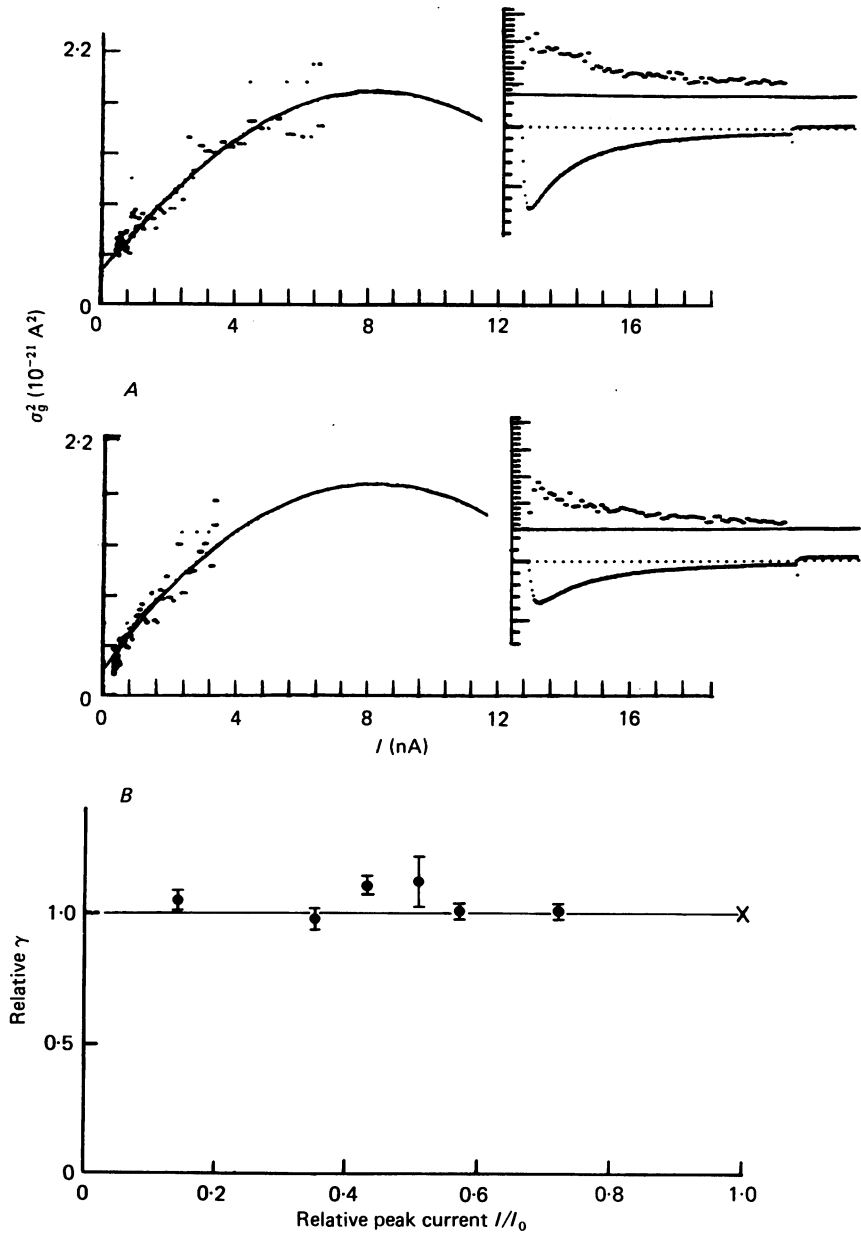


Fig. 2. *A*, effect of prepulses on variance-mean relationship. 50 ms prepulses to  $-105 \text{ mV}$  (upper) and  $-70 \text{ mV}$  (lower) were given before depolarizations to  $-5 \text{ mV}$ . Both curves are drawn according to eqn. (2) with  $i = 0.47 \text{ pA}$ ,  $N = 30,000$ ,  $\gamma = 6.9 \text{ pS}$ . Node 38. Insets show the time courses of the variance (upper trace;  $2 \times 10^{-22} \text{ A}^2/\text{small division}$ ) and mean current ( $1 \text{ nA}/\text{small division}$ ). *B*, normalized  $\gamma$  values from six fibres obtained with 50 ms prepulses to between  $-71$  and  $-55 \text{ mV}$ . Each point represents a different fibre with the  $\gamma$  value normalized to the control value  $\gamma_0$  obtained with prepulses to  $-105 \text{ mV}$ . Peak currents  $I$  were normalized to the control values  $I_0$ . Error bars are standard errors of  $\gamma$  with  $N$  constrained to the control value.

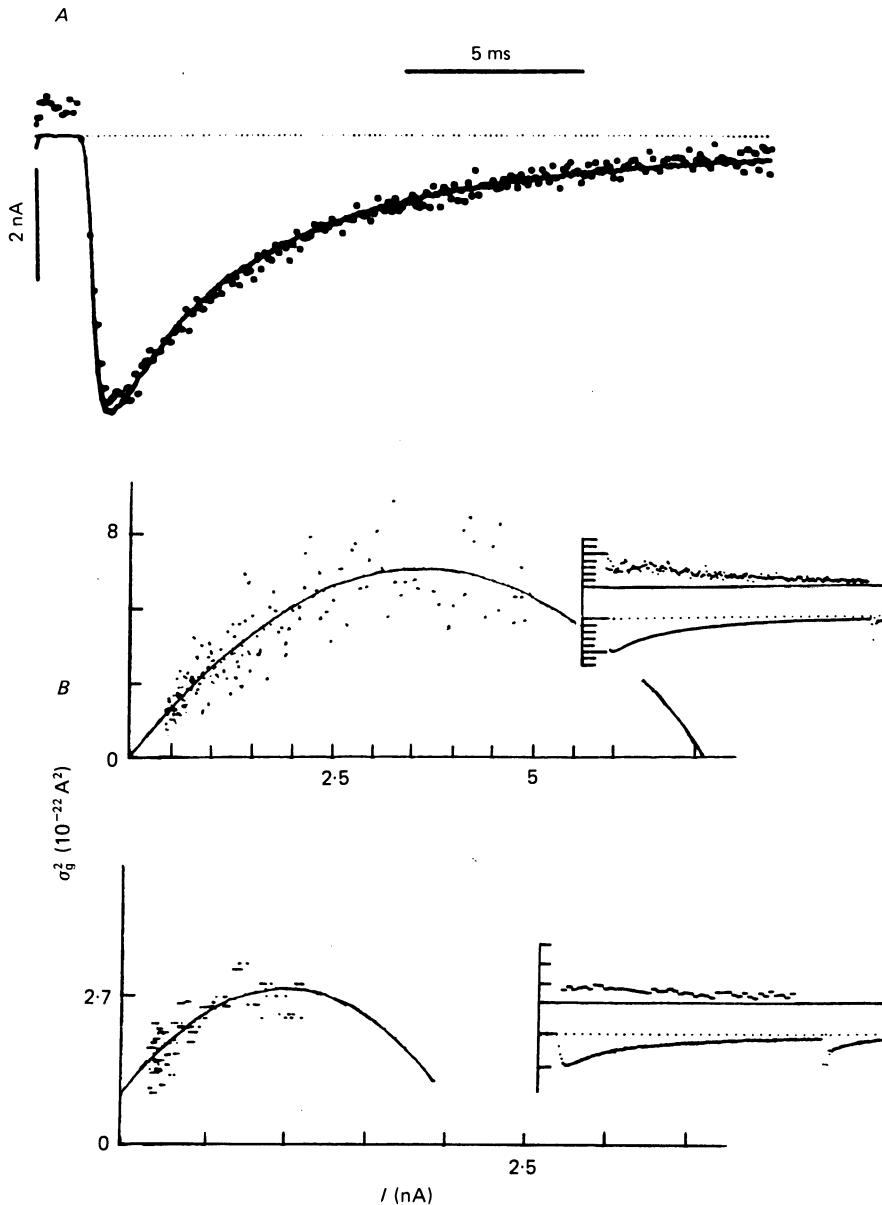


Fig. 3. *A*, comparison of sodium current records before (continuous trace) and during application of 8 nM-TTX. Depolarizations to  $-5$  mV preceded by prepulses to  $-105$  mV. The current in TTX was shifted by  $0.1$  nA (note the change in the initial base lines) and scaled by a factor of  $5.6$ . *B*, effect of partial block by TTX on the variance-mean relationship. Control (upper) and after application of 8 nM-TTX (lower). The control data were taken immediately before application of TTX. Both curves are drawn with  $i = -0.36$  pA, but in the upper trace  $N = 21,900$  while in the lower trace  $N = 4200$ . Node 24. Calibrations of insets are the same as in Fig. 2*A*.

maximum, and the value of  $N$  was  $26,000 \pm 11,000$ . The control value was  $N = 36,000 \pm 7000$  with prepulses to  $-105$  mV. The  $\gamma$  values plotted in Fig. 2B were obtained by constraining  $N$  to the control values.

*Partial block by toxins.* Fig. 3 shows the effect of a partial block by TTX. The time course of the current is not affected, and the variance-mean relationship can be

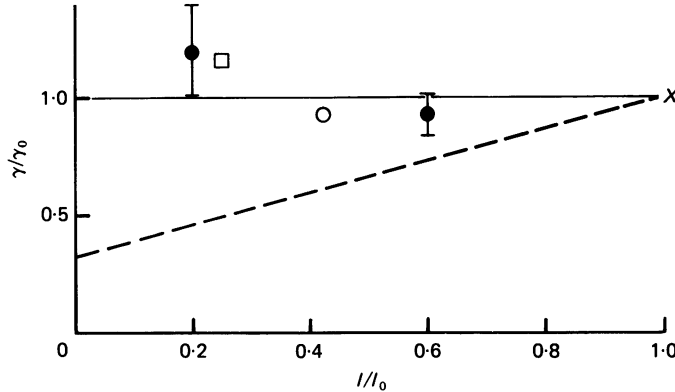


Fig. 4. Normalized  $\gamma$  values as a function of peak current with partial block by 4 and 8 nM-TTX (filled symbols) or 2.5 nM-STX (open symbols) in three experiments.  $\gamma$  and  $I$  were normalized to the values  $\gamma_0$  and  $I_0$  obtained with no TTX. Prepulses to  $-105$  mV for 50 ms; test pulse to  $-5$  mV. Error bars show the standard error of  $\gamma$  in unconstrained least-square fits. The values in STX were obtained from the covariance, and error estimates are not available; however, the errors are expected to be similar in size to the TTX values. The dashed line is the prediction of a theory that assumes a positive correlation in the gating of channels (eqn. (4)).

TABLE 1. Effect on  $\gamma$  and  $N$  of small concentrations of TTX and STX. Toxin concentrations are given in nM;  $\gamma$  in pS;  $N$  in thousands; peak current during the depolarizations to  $-5$  mV, in nA. Asterisks indicate values obtained from the covariance

Node	Toxin	$\gamma$	$N$	$I_{\text{peak}}$
24	Control	$6.6 \pm 0.3$	$23 \pm 2$	5.1
	4 TTX	$6.2 \pm 0.5$	—	3.0
	8 TTX	$8.0 \pm 1.3$	$5 \pm 1$	0.9
32	Control	6.4*	42*	6.2
	2.5 STX	5.9*	14*	2.6
36	Control	6.6*	17*	6.6
	2.5 STX	7.6*	8*	1.8

described by the same value of  $i$  as shown by the constrained fit in the Figure. In experiments on three fibres (Fig. 4) no significant change in  $\gamma$  occurred while the peak current was reduced by TTX and STX to as little as 1/5 of normal. The large uncertainty of the  $\gamma$  values in the Figure resulted in part from the necessity of unconstrained fits to yield values for both  $\gamma$  and  $N$ . As can be seen in Table 1, values of  $N$  were reduced by the toxins roughly in proportion to the reduction in peak current. The toxins therefore seem to reduce the current by removing some of the channels from the population represented by  $N$ .

*Effect of low pH.* At low pH the single channel current was reduced, but the same value of  $N$  could be used in fitting the variance-mean relationship from both the

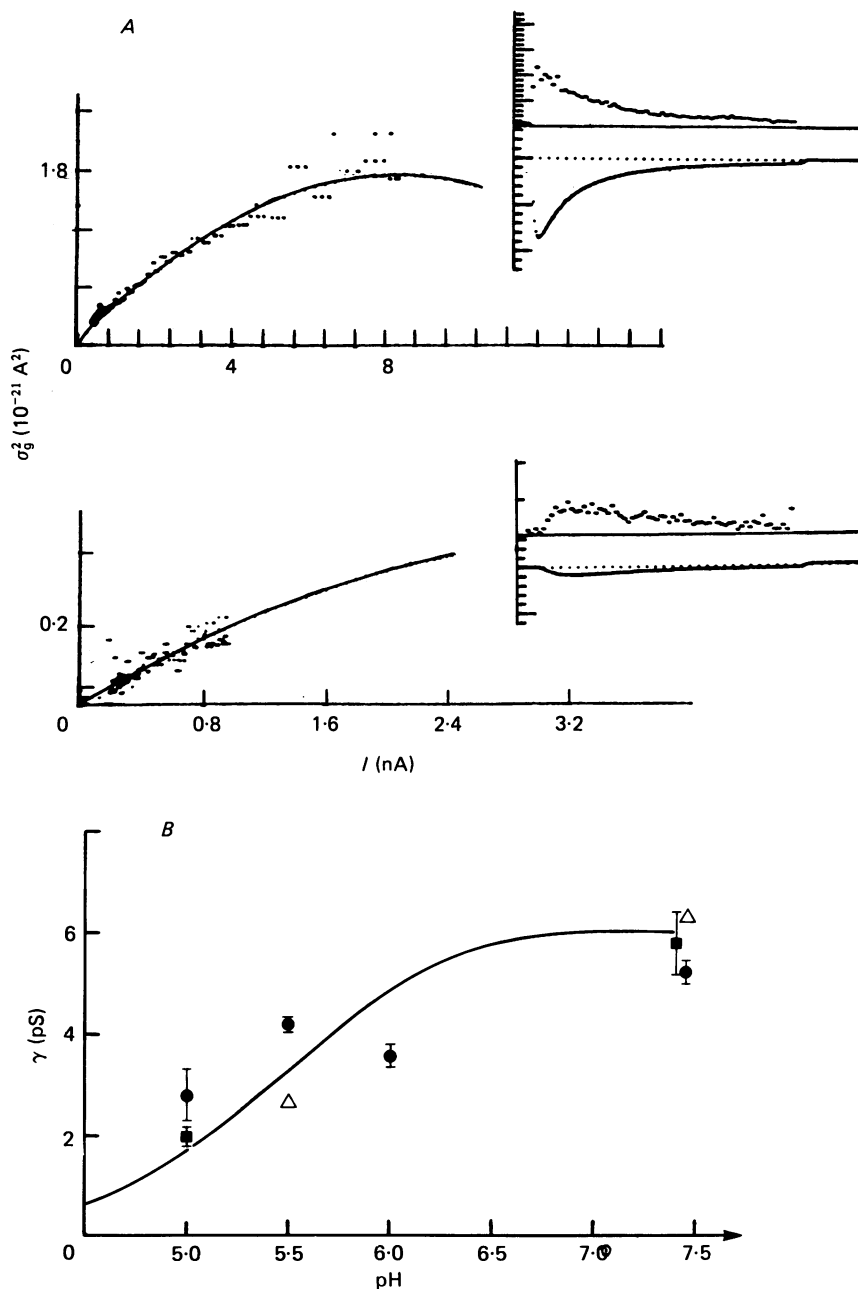


Fig. 5. pH dependence of single-channel conductance. *A*, variance-mean relationship for node 32 at pH = 7.4 (upper) and 5.0 (lower) from depolarizations to  $-5 \text{ mV}$ . The fitted curves are for  $i = -0.39$  and  $-0.19 \text{ pA}$ , respectively. The value  $N = 46,000$  was the same for both curves. Calibrations of the insets are the same as in Fig. 2*A*. *B*,  $\gamma$  as a function of pH. Filled symbols: values and standard errors from the variance-mean relationship in nodes 12 (■) and 32 (●). Open symbols, determinations using the covariance in node 30. At the lower pH values,  $N$  was constrained to the value at pH = 7.4. The continuous curve corresponds to the titration of a single site with  $\text{p}K_a = 5.4$ .

control and low pH currents (Fig. 5). At the test potential of  $-5$  mV, the theory of Woodhull (1973) would predict a titration of  $\gamma$  with  $\text{pk}_a = 5.4$ . The observed  $\gamma$  values are plotted in Fig. 5B as a function of pH and are seen to be consistent with the theory's prediction. As can be seen in Table 2, the decrease in  $\gamma$  does not account for all of the reduction in the peak current. Estimates for  $N$  at low pH had large uncertainties; meaningful values of  $N$  could be determined only in node 32. These values show a small decrease of  $N$  with decreasing pH which has little statistical significance. The peak number of channels open  $N_{\text{peak}} = I_{\text{peak}}/i$  showed a marked decrease, on the other hand, which would be expected from a shift of the activation curve at low pH.

TABLE 2. Effect of low pH on  $\gamma$  and  $N$ . Values are given in the same units as in Table 1, with  $N_{\text{peak}} = I_{\text{peak}}/i$  being the peak number of channels open, in thousands. The asterisk denotes  $\gamma$  value obtained from the covariance

Node	pH	$\gamma$	$N$	$I_{\text{peak}}$	$N_{\text{peak}}$
12	7.4	$5.8 \pm 0.6$	35	6.3	14
	5.0	$2.0 \pm 0.1$	—	2.4	6
30	7.4	$6.3 \pm 0.2$	$31 \pm 3$	9.4	21
	5.5	2.7*	—	2.1	11
32	7.4	$5.1 \pm 0.2$	$51 \pm 3$	8.7	24
	6.0	$3.6 \pm 0.22$	$43 \pm 7$	4.1	16
	5.5	$4.2 \pm 0.1$	—	3.7	13
	5.0	$2.8 \pm 0.5$	—	1.0	5

*Low external sodium.* In two fibres  $\gamma$  was measured with low external sodium concentrations, with tetramethylammonium as an impermeant substitute. In node 14  $\gamma$  was reduced from the control value of 5.6 to 4.1 pS in 55 mM-sodium while  $E_{\text{Na}}$  changed from +65 to +45 mV; both  $\gamma$  determinations were made at  $-5$  mV. In node 43  $\gamma$  changed from 6.9 to 2.3 pS in 20 mM-sodium with the  $E_{\text{Na}}$  values being +58 and +20 mV. The  $\gamma$  determinations were made at  $-15$  and  $-30$  mV, respectively. Values for  $N$  could not be obtained in the low sodium solutions.

#### DISCUSSION

*Three time scales of channel block.* In these experiments the various means of reducing the sodium conductance resulted in different effects on the parameters  $\gamma$  and  $N$ . These effects can be explained on the basis of the different durations of the blocked state of the channel. The theory of Woodhull (1973) postulates that the block by  $\text{H}^+$  is an all-or-none process, but is extremely rapid. Since the lifetime of the blocked state would not be expected to be much longer than the transit time of an ion through the channel, of the order of 100 ns, the fluctuations due to this process would not have been observed in those experiments. The resulting value of  $\gamma$  is therefore reduced, being in effect an average of  $\gamma$  over an interval of about 30  $\mu\text{s}$  determined by the filter band width of 5 kHz.

Two other time scales can be distinguished for slower blocking processes. Let  $\tau$  be the time constant for the relaxation of the blocking process. If  $\tau$  is greater than the



temporal resolution of the current recording but is small compared to the pulse repetition interval  $T$ , the fluctuations from channel block will be indistinguishable from the spontaneous gating fluctuations, and  $i$  and  $N$  will equal the actual single-channel current and number of channels. The inactivation of channels with prepulses occurs on this intermediate time scale, with the inactivation time constant  $\tau_h \leq 30$  ms being much shorter than  $T = 400$  ms. From pulse to pulse the population of channels that are not inactivated and therefore can be opened is randomized and, in effect, chosen anew by the inactivation process with probability  $p_N$ . From the population of available channels, a fraction  $p$  are then 'chosen' to be opened. This sequence of two Bernoulli trials is equivalent to a single one with the probability being the product  $p_N p$ . Hence the effect of depolarizing prepulses is expected to be a reduction in the probability of channels being open while the apparent total number of channels remains constant.

An example of the longest time scale, on the other hand, is provided by the block by TTX and STX. In this case  $\tau$ , calculated from the rate constants at 16 °C of Wagner & Ulbricht (1975) and Ulbricht & Wagner (1975), would be in the range 10–68 sec, much larger than the repetition interval. Relatively little rearrangement of the population of available channels would be expected to occur between pulses. The current fluctuations from pulse to pulse therefore would reflect the size of the nearly fixed population of unblocked channels, rather than the total number of channels. Such a reduction of  $N$  with toxin block is observed. (It may be noted that by suitable choices of  $T$  the binding rates of channel-blocking compounds might be measured by this technique.)

*H<sup>+</sup> has both gating and permeation effects.* Drouin & Neumcke (1974) have presented an alternative theory to that of Woodhull for the pH block of channels. Unlike Woodhull's theory, which places the binding site part way through the membrane field, Drouin & Neumcke postulate a site on the outer surface of the membrane that has the lower  $pK_a$  value of 4.6. However, when the effect on the local sodium concentration of the titratable surface charge is also included, their prediction for the pH dependence of  $\gamma$  is essentially the same at  $-5$  mV as the titration curve in Fig. 5B. The data do not allow discrimination between these two theories.

Both theories include shifts in the channel gating as well as ion permeation effects due to  $H^+$ . The results reported here are consistent with such a dual effect of low pH, and argue against other possible theories in which the reduction of the sodium current is entirely due to changes in the gating of channels. It should be remembered, however, that the distinction in these experiments between a reduction in  $\gamma$  and a change in the gating properties of the channels is based only on the time scale of the effects. The apparent decrease in  $\gamma$  could have arisen from a very rapid ( $< 30 \mu\text{s}$  relaxation time) gating process that becomes prominent at low pH. The simplest explanation, however, is that low pH has a direct effect on ion permeation.

*Independence of channel gating.* Various authors have proposed theories of channel gating that postulate interactions among channels. The theories of Tille (1965); Adam (1960) and Hill & Chen (1971) assume cooperative interactions among channels that form a regular array in the membrane, and Tille has shown that the high order kinetics of the Cole & Moore (1960) hyperpolarization delay could be explained by such a theory. Changeux, Thiéry, Tung & Kittel (1967) have presented a theory of

cooperativity among membrane-bound enzymes which, if applied to ionic channels, would explain the steep voltage-dependence of activation without requiring a large dipole moment in each channel macromolecule. Hill & Chen (1971) recognized the relatively low density of potassium channels in the nerve membrane and considered interactions within small, widely dispersed patches of channels. Fluctuation analysis now allows tests to be made for gating interactions of these kinds.

One test, with a negative result, for interactions among potassium channels has already been reported (Sigworth, 1979). For sodium channels the effect on  $\gamma$  of a partial block by TTX and STX is a test for the correlations in gating that would arise from interactions between the gating mechanisms of channels. In these experiments a positive or negative cooperativity would have caused the single-channel conductance to appear larger or smaller, respectively, at high conductance levels as compared to the condition of partial toxin block. This effect would arise because toxin block or inactivation would render some of the channels 'invisible' to the fluctuation measurement. Assuming that the only interactions among channels are short-range ones, the blockage of a fraction of the channels would cause the remaining channels to show smaller correlations due to interactions. The relative constancy of  $\gamma$  with toxin block (Fig. 4) and depolarizing prepulses (Fig. 2*B*) argues against such interactions among sodium channels.

A specific theory involving a gating interaction among sodium ion pores is suggested by the toxin-binding results of Catterall & Morrow, (1978), who found a three-times higher density of STX binding sites than scorpion toxin (ScTX) sites in neuroblastoma cells. One of many possible explanations for this would be that each sodium-channel gating system, with an ScTX site, controls three pores, each having an STX site. From the standpoint of gating statistics, this model is equivalent to total, positive cooperativity within groups of three channels. Its prediction is a linear relationship between  $\gamma$  and the peak current with  $\gamma$  decreasing to  $\frac{1}{3}$  of the control at maximum block, shown as a dashed line in Fig. 4. This prediction is not consistent with the relatively constant  $\gamma$  value that was observed.

A derivation of the prediction will now be given. For generality, assume that each sodium channel macromolecule contains one 'gating system' that controls  $m$  pores, each independently blockable by STX. As before, the blocking relaxation time is assumed to be long compared to the time-scale of the fluctuation measurement  $T$ . The mean current and variance from  $N$  gating systems would depend on the expectation values obtained with the various values of the single channel current  $i$ ,

$$\begin{aligned} I &= N \langle i \rangle p \\ \sigma_i^2 &= N \langle i^2 \rangle p(1-p) \end{aligned} \quad (2)$$

where the expectation values

$$\begin{aligned} \langle i \rangle &= \sum_{k=1}^m r_k i_k \\ \langle i^2 \rangle &= \sum_{k=1}^m r_k i_k^2 \end{aligned}$$

depend on the degree of toxin block through the probabilities  $r_k$  of being in the current stages  $i_k$ , and

$$i_k = \frac{k}{m} i_0$$

is proportional to the number  $k$  of unblocked pores per gating system. From the assumption of independent toxin binding to each pore, with each pore having probability  $r$  of being unblocked,

$$\begin{aligned}\langle i \rangle &= r i_0 \\ \langle i^2 \rangle &= \frac{i_0}{m} (r - r^2 + m r^2)\end{aligned}\quad (3)$$

The apparent single channel current calculated from the fluctuation measurement is

$$i' = \frac{\langle i^2 \rangle}{\langle i \rangle} = i_0 \left( \frac{1}{m} + \frac{m-1}{m} r \right)\quad (4)$$

When no toxin is present,  $r = 1$  and the full current associated with each gating system is observed. As  $r$  decreases toward zero with increasing block, the apparent single channel current  $i'$  approaches  $i_0/m$ , the current through a single pore. The linear relationship between  $r$  and  $i'$  with  $m = 3$  is drawn as a dashed line in Fig. 4. The data are consistent with the constant  $\gamma$  line ( $P > 0.2$ ) but are significantly far from the prediction of this theory ( $P < 0.01$  by Student's  $t$  test).

*Other possible forms of cooperativity.* Besides a direct, allosteric interaction between channels like the one analysed above, two other kinds of interactions between channels can be imagined. Both would result from local perturbations in the membrane electric field changing the activation of channels. In one case, the perturbations arise from the ion flow either in nearby channels or in the membrane as a whole. The other involves dipole-dipole interactions between the gating charges of the channels. My experiments were not very sensitive to interactions of these kinds because they were performed at a potential where the activation and inactivation processes have low voltage sensitivity.

Other evidence, however, suggests that these interactions are small. First, the gating kinetics are not affected by changes in the sodium concentration (Hodgkin & Huxley, 1952; Hille, 1966) or by small doses of TTX (Fig. 3A; also, see Takata, Moore, Kao & Fuhrman, 1966; Hille, 1968) which would affect ion flow. Series-resistance or other interactions between current and gating would be expected to have different effects on gating kinetics as the current is reduced by these means. Secondly, since gating-current experiments have shown that most of the gating charge movement is immobilized by inactivation (Armstrong & Bezanilla, 1977; Meves & Vogel, 1977; Nonner, 1979) similar voltage dependences of activation at different levels of inactivation would argue against gating-charge interactions.

Studies on channel properties from conductance fluctuations have always assumed the independence of channel gating, and only in an artificial membrane system (Kolb & Bamberg, 1977) has evidence for possible local interactions between channels been seen. The experiments reported here show no evidence for interactions among sodium channels.

I am grateful to Dr C. F. Stevens for the privilege of working in his laboratory, and to Dr S. R. Levinson, who pointed out to me the issue of interactions among channels. This work was supported by U.S.P.H.S. grant no. 12962.

## REFERENCES

- ADAM, G. (1960). In *Physical Principles of Biological Membranes*, ed. F. SNELL, J. WOLKEN, G. IVERSON & J. LAM. New York: Gordon and Breach.
- ARMSTRONG, C. & BEZANILLA, F. (1977). Inactivation of the sodium channel II. Gating current experiments. *J. gen. Physiol.* **70**, 567-590.
- CATTERALL, W. A. & MORROW, C. (1978). Binding of saxitoxin to electrically excitable neuroblastoma cells. *Proc. natn. Acad. Sci. U.S.A.* **75**(1), 218-222.
- CHANGEUX, J.-P., THIÉRY, J., TUNG, Y. & KITTEL, C. (1967). On the cooperativity of biological membranes. *Proc. natn. Acad. Sci. U.S.A.* **57**, 335-341.
- COLE, K. S. & MOORE, J. W. (1960). Potassium ion current in the squid giant axon: dynamic characteristic. *Biophys. J.* **1**, 1-14.
- DROUIN, H. & NEUMCKE, B. (1974). Specific and unspecific charges at the sodium channels of the nerve membrane. *Pflügers Arch.* **351**, 207-229.
- HILL, T. L. & CHEN, Y.-D. (1971). On the theory of ion transport across the nerve membrane, II. Potassium ion kinetics and cooperativity (with  $x = 4$ ). *Proc. natn. Acad. Sci. U.S.A.* **68**, 1711-1715.
- HILLE, B. (1966). The common mode of action of three agents that decrease the transient change in sodium permeability in nerves. *Nature, Lond.* **210**, 1220-1222.
- HILLE, B. (1968). Pharmacological modifications of the sodium channels of frog nerve. *J. gen. Physiol.* **51**, 199-219.
- HODGKIN, A. L. & HUXLEY, A. F. (1952). Currents carried by sodium and potassium ions through the membrane of the giant axon of *Loligo*. *J. Physiol.* **116**, 449-472.
- KOLB, H.-A. & BAMBERG, E. (1977). Influence of membrane thickness and ion concentration on the properties of the gramicidin A channel: autocorrelation, spectral power density, relaxation and single-channel studies. *Biochim. biophys. Acta* **464**, 127-141.
- MEVES, H. & VOGEL, W. (1977). Inactivation of the asymmetrical displacement current in giant axons of *Loligo forbesi*. *J. Physiol.* **267**, 377-393.
- NONNER, W. (1979). Does immobilization of gating charge reflect properties of Na inactivation in myelinated nerve? *Biophys. J.* **25**, 194a.
- SIGWORTH, F. (1979). The Cole-Moore delay: cooperativity among potassium channels? *Biophys. J.* **25**, 196a.
- SIGWORTH, F. (1980). The variance of sodium current fluctuations at the node of Ranvier. *J. Physiol.* **307**, 97-129.
- TAKATA, M., MOORE, J. W., KAO, C. Y. & FUHRMAN, F. A. (1966). Blockage of sodium conductance increase in lobster giant axon by tarichatoxin (tetrodotoxin). *J. gen. Physiol.* **49**, 977-988.
- TILLE, J. (1965). A new interpretation of the dynamic changes of the potassium conductance in the squid giant axon. *Biophys. J.* **5**, 163-171.
- ULBRICHT, W. & WAGNER, H. (1975). Influence of pH on rate of tetrodotoxin action on myelinated nerve fibres. *J. Physiol.* **252**, 185-202.
- WAGNER, H. H. & ULBRICHT, W. (1975). Rates of saxitoxin action and of saxitoxin-tetrodotoxin interaction at node of Ranvier. *Pflügers Arch.* **359**, 297-315.
- WOODHULL, A. (1973). Ionic Blockage of Sodium Channels in Nerve. *J. gen. Physiol.* **61**, 687-708.